

Quantum computing simulation of ${}^6\text{Li}$ with the coupled cluster method

Author: Miquel Carrasco Codina

Facultat de Física, Universitat de Barcelona, Diagonal 645, 08028 Barcelona, Spain.

Advisor: Arnau Rios Huguet

Abstract: There is an increasing interest to develop quantum circuits capable of performing many-body quantum simulation motivated by their scaling advantages against classical devices. We present an analysis of the performance of the unitary coupled cluster method for the ${}^6\text{Li}$ nucleus in the shell model framework. Our work consists of several tests aimed to establish proper criteria to improve its performance. By isolating the main aspects of the UCC *ansatz*, we are able to understand their effect on the simulation. Consequently, we identify different ways to optimise the ${}^6\text{Li}$ simulation by reducing the operators used and choosing efficient Trotter number and reference state.

I. INTRODUCTION

The study of the structure and dynamics of atomic nuclei is characterized by the complexity of the nuclear interactions between its components, protons and neutrons. This complexity sets a huge challenge for nuclear physics, and there has always been an interest to pursue efficient high precision simulations. One of the biggest challenges for nuclear physics is the exponential scaling of computing resources with the Hilbert space dimension using classical computers [1]. However, quantum computing seems to be a promising way to solve large many-body quantum problems, thanks to the ability to describe the Hilbert space scaling linearly with its dimension [2].

For the last years many quantum simulation methods have been developed and studied and in this work we test one of the most promising, the *unitary coupled cluster* method (UCC). Our approach to the UCC method is part of a greater framework aimed at comparing multiple similar methods such as the ADAPT [3] and the RODEO [4]. However, here we focus on the performance of the UCC method used to simulate the ${}^6\text{Li}$ nucleus described by the nuclear shell model.

II. THE NUCLEAR SHELL MODEL

The nuclear shell model is a theory based on the idea that nucleons occupy certain energy levels and form shells similar to the atomic model [5, 6]. This model successfully describes how certain numbers of nucleons lead to very stable shells. It postulates that closed shells do not affect the dynamics of the particles that occupy the so-called valence nucleons. In this context the formulation of the nuclear shell model in second quantisation is often given by a single-particle basis defined by the quantum numbers of the valence nucleons $njmt_z$: the principal quantum number (n), the orbital angular momentum (l), the total angular momentum (j), the magnetic quantum number m and the third component of the isospin (t_z).

Second quantisation is a formulation to describe many-body states as a combination of the single particle states

in the so-called Fock space [7]. Creation \hat{a} and annihilation \hat{a}^\dagger operators are the building blocks of the formalism, creating or destroying particles in certain states. In second quantisation, the nuclear shell model Hamiltonian takes account of single-particle energies and the two-body interaction:

$$\hat{H}_{eff} = \sum_i \varepsilon_i \hat{a}_i^\dagger \hat{a}_i + \frac{1}{4} \sum_{ijkl} \bar{v}_{ijkl} \hat{a}_i^\dagger \hat{a}_j^\dagger \hat{a}_l \hat{a}_k, \quad (1)$$

where ε_i is the energy of the single-particle state and \bar{v}_{ijkl} is the antisymmetrised two-body matrix element of the Hamiltonian.

The elements of matrix of the Hamiltonian that we use are provided by the Cohen-Kurath interaction, a phenomenological interaction based on empirical results of several nucleus within the p shell [8].

A. The ${}^6\text{Li}$ nucleus

This work focuses on the implementation of the UCC method for the ${}^6\text{Li}$ nucleus. This many-body system consists only of two particles in the valence p shell: a neutron and a proton [5]. This happens because the s shell of the nucleus is full of particles, with two protons and two neutrons, analogous to the ${}^4\text{He}$ nucleus.

The two valence neutrons can only occupy the 6 different single-particle states shown in Fig. 1, based on their quantum numbers $njmt_z$. In particular, both $n = 0$ and $l = 1$ are shared by all states, since we consider that the nucleons can only be in the $0p$ shell. In addition, the third component of the isospin is shared for protons, with $t_{z,p} = \frac{1}{2}$, and neutrons share $t_{z,n} = -\frac{1}{2}$. That means a proton and a neutron can occupy states with the same $njlm$ numbers.

Meanwhile, the many-body states of the entire nucleus are Slater determinants using the discussed single-particle states. The different determinants must share the same quantum magnetic number (M). Since the total angular momentum of ${}^6\text{Li}$ is $J = 1$ we can choose between $M = -1, 0$ or 1 . We simulate the nucleus with $M = 0$ because it is the most general choice, since all

$0p_{1/2}$		<u>5</u>	<u>4</u>	
$0p_{3/2}$	<u>3</u>	<u>2</u>	<u>1</u>	<u>0</u>
m	$-\frac{3}{2}$	$-\frac{1}{2}$	$\frac{1}{2}$	$\frac{3}{2}$

FIG. 1: Schematic representation of the single-particle states available in the $0p$ shell. The labels in the left are written as: nl_j . Values of m are shown in the bottom.

nuclei with an even number of nucleons can have this value. All the resulting Slater determinants that fulfill this property are shown in Table I.

III. COUPLED CLUSTER THEORY

The *coupled cluster* (CC) method appeared in 1960 as an approximation to calculate nuclear binding energies [9] and was successful, being used, not only in nuclear physics, but also to solve electronic structure problems. Consequently, CC theory has been constantly developed and implemented in several quantum mechanics areas. The cornerstone of the CC formulation is the so-called *ansatz*, the initial wave function guess that can be written as follows:

$$|\Phi_{CC}\rangle = e^{\hat{T}}|0\rangle, \quad (2)$$

where $|0\rangle$ is a known reference state of choice and \hat{T} is the so-called cluster operator,

$$\hat{T} = \sum_i \hat{T}_i. \quad (3)$$

\hat{T}_i operators consists of a linear combination of many-body fermionic excitations:

$$\hat{T}_i = \sum_{pq\dots rs\dots} \theta_{pq\dots}^{rs\dots} \hat{\tau}_{pq\dots}^{rs\dots}, \quad (4)$$

where $\hat{\tau}_{pq\dots}^{rs\dots}$ are excitation operators that brings particles from p, q, \dots occupied states to r, s, \dots empty states, and $\theta_{pq\dots}^{rs\dots}$ their amplitudes (or weights).

Although the CC method was not originally designed as a variational method, the CC *ansatz* can be used with the variational principle. The minimisation of the energy expectation value depending on the parameters θ_k leads to the ground state energy:

$$E_{CC} = \min_{\theta_{pq\dots}^{rs\dots}} \langle \Phi_{CC} | \hat{H} | \Phi_{CC} \rangle = \min_{\theta_{pq\dots}^{rs\dots}} \langle 0 | e^{-\hat{T}} \hat{H} e^{\hat{T}} | 0 \rangle \quad (5)$$

In the NISQ era of quantum computing, the variational principle is often used to approximate energies with the so-called variational quantum eigensolvers (VQE). VQE

$ v_i\rangle$	$ j_p, m_p, j_n, m_n\rangle$
$ v_1\rangle$	$ \frac{1}{2}, \frac{1}{2}, \frac{1}{2}, \frac{1}{2}\rangle$
$ v_2\rangle$	$ \frac{1}{2}, -\frac{1}{2}, \frac{3}{2}, \frac{1}{2}\rangle$
$ v_3\rangle$	$ \frac{1}{2}, \frac{1}{2}, \frac{1}{2}, -\frac{1}{2}\rangle$
$ v_4\rangle$	$ \frac{1}{2}, \frac{1}{2}, \frac{3}{2}, -\frac{1}{2}\rangle$
$ v_5\rangle$	$ \frac{3}{2}, -\frac{3}{2}, \frac{3}{2}, \frac{3}{2}\rangle$
$ v_6\rangle$	$ \frac{3}{2}, -\frac{1}{2}, \frac{1}{2}, \frac{1}{2}\rangle$
$ v_7\rangle$	$ \frac{3}{2}, -\frac{1}{2}, \frac{3}{2}, \frac{1}{2}\rangle$
$ v_8\rangle$	$ \frac{3}{2}, \frac{1}{2}, \frac{1}{2}, -\frac{1}{2}\rangle$
$ v_9\rangle$	$ \frac{3}{2}, \frac{1}{2}, \frac{3}{2}, -\frac{1}{2}\rangle$
$ v_{10}\rangle$	$ \frac{3}{2}, \frac{3}{2}, \frac{3}{2}, -\frac{3}{2}\rangle$

TABLE I: The 10 Slater determinants of the many-body basis for the ${}^6\text{Li}$ nucleus. States are labeled by the total angular momentum of the proton (j_p), the magnetic quantum number of the proton (m_p), the total angular momentum of the neutron (j_n) and the magnetic quantum number of the neutron (m_n).

algorithms consist of a quantum circuit that performs some operations on a reference state depending on several parameters and a classical computer that minimises the measured energy of the final state according to these parameters.

Among all variational CC methods, the *unitary coupled cluster* (UCC) *ansatz* has emerged as a powerful method for quantum computers. The UCC *ansatz* is build from unitary exponential operators, which are efficiently implemented in quantum algorithms [10]. In order to make the cluster operator unitary, the excitation operators in the exponential must be antihermitian. The UCC cluster operator is the exponential of an antihermitian operator $\hat{\sigma}$. In particular, we use a sum of two-body excitation operators which can be written in second quantisation as:

$$\hat{\sigma} = \sum_{pqrs} \hat{T}_{rs}^{pq} = \sum_{pqrst} \theta_{rs}^{pq} (\hat{a}_p^\dagger \hat{a}_q^\dagger \hat{a}_r \hat{a}_s - \hat{a}_r^\dagger \hat{a}_s^\dagger \hat{a}_p \hat{a}_q), \quad (6)$$

where p, q, r and s are single-particle labels. Thus, from Eq. (5), we can write the UCC energy using the defined operators: $E_{UCC} = \min_{\theta} \langle 0 | e^{-\hat{\sigma}} H e^{\hat{\sigma}} | 0 \rangle$.

We only use the \hat{T}_{rs}^{pq} operators that maintain the magnetic quantum number of the nucleus $M = 0$ and the ones that do not annihilate and create the same particles. Furthermore, \hat{T}_{rs}^{pq} operators are anti-symmetric, which means that $\hat{T}_{rs}^{pq} = -\hat{T}_{rs}^{qp} = -\hat{T}_{sr}^{pq}$. Our operator pool does not include the 4 possible operators with the same labels in different orders, *e.g.* we have \hat{T}_{rs}^{pq} but not \hat{T}_{rs}^{qp} , \hat{T}_{sr}^{pq} or \hat{T}_{sr}^{qp} . Consequently, our operator pool consists of 45 operators that fulfill the previous criteria.

In order to implement the cluster operator using quantum gates, we want the cluster operator to be a product of $e^{\hat{T}_{rs}^{pq}}$ exponentials. Since the exponential of a sum of

non-commuting matrices cannot be separated in a product of exponentials ($e^{\hat{A}+\hat{B}} \neq e^{\hat{A}}e^{\hat{B}}$) we need to introduce an approximation called the Trotter decomposition. The Trotter decomposition can be written as:

$$e^{\hat{\sigma}} = e^{\sum_{pqrs} \hat{T}_{rs}^{pq}} \approx \left(\prod_{pqrs} e^{\frac{\hat{T}_{rs}^{pq}}{t}} \right)^t + \mathcal{O}\left(\frac{1}{t}\right), \quad (7)$$

where t is the Trotter number [11]. This is an important feature when it comes to building the *ansatz* since using a large t reduces the error of the approximation, but requires to linearly increase the demanding quantum computation resources. This is because adding one more layer of operators in the *ansatz* translates to one more layer of quantum gates in the circuit. Also, using this approximation we need to take into account the ordering of the operators in the product, since $e^{\hat{A}}e^{\hat{B}} \neq e^{\hat{B}}e^{\hat{A}}$. This is also another key feature of the UCC *ansatz* and we will discuss its impact later.

It is possible to build a quantum circuit that applies the Trotter decomposition of the exponential of the UCC operator to the reference state and measures the energy expectation value according to several parameters. Along with the quantum device we also need a classical minimization algorithm, calling the energy function over and over until it finds the values of the UCC parameters θ_{rs}^{pq} , in addition to the ground state energy, this method provides the ground state itself.

IV. UCC PERFORMANCE FOR THE ${}^6\text{Li}$ NUCLEUS

In this section we put the UCC method to test using classical computation to understand how can it be optimised to perform in a quantum device.

To establish a benchmark of the precision and functionality of the method in this section we provide two observables comparing the ground state energy E_{UCC} and the ground state wave function Φ_{UCC} from the UCC predictions with the results computed by the diagonalisation of the Hamiltonian matrix, E_0 and ϕ_0 . These observables are the relative error of the ground energy level $\epsilon_E = \left| \frac{E_{UCC} - E_0}{E_0} \right|$ and the infidelity $I = 1 - |\langle \Phi_0 | \Phi_{UCC} \rangle|^2$. In addition, we quantify the efficiency of the method using the number of function calls of the optimiser algorithm N_{fcall} .

In particular, we use `pyhon`'s libraries to diagonalise the Hamiltonian matrix and `scipy`'s minimisation function, with the Broyden–Fletcher–Goldfarb–Shanno method (BFGS) to minimise the energy function.

A. Default procedure

The first test we performed consisted of using the 45 operators to build the *ansatz*, along with the first state

	E_{UCC} (MeV)	ϵ_E	I	N_{fcall}
45 operators	-5.5567831	2.2×10^{-8}	2.4×10^{-8}	1288
9 operators	-5.5567831	2.2×10^{-8}	2.5×10^{-8}	280

TABLE II: Results of the UCC *ansatz* minimisation using the default 45 operators and the reduced 9 operators.

of the many-body basis ($|v_1\rangle$) as the reference state. The optimisation of the energy was successful, returning the results presented in Table II.

At first sight, the results are promising. Both ϵ_E and I have a near zero value, which indicates the high overlap the final state has with the ground state. Although the BFGS optimiser could continue with the minimisation, we established an upper limit for the relative error at $\epsilon_E \geq 1 \times 10^{-9}$ that cannot be surpassed. This precision is much higher than the currently used in nuclear physics [12]. This is maintained through the entire work.

B. Optimisation

There are three main aspects of the UCC *ansatz* that can affect the simulation, in terms of precision, computational time and resources: the number and ordering of the operators (\hat{T}), the reference state ($|0\rangle$) and the Trotter number (t).

Before going any further, we realise that a large number of operators we use to perform the calculus are unnecessary. Since we use all 45 operators from the operator pool, the optimiser algorithm has to work with 45 different parameters, making the process hard computationally. Several parameters have very small relative values, due to the presence of operators with no effect on the reference state. Furthermore, we also observe that the final values of θ come in pairs with opposite sign.

Next, we select only operators that have some effect on the reference state. This reduces significantly the number of operators down to 9 of them for any state of the basis, due to there is only 9 possible excitations that maintain $M = 0$ for each state.

The results using this reduced operator pool are shown in the second line of Table II. As we can see, there is great improvement in N_{fcall} , that has reduced almost by a fourth, while getting the same results. From now on, we will use this selection of 9 operators to perform further tests.

The main features of the *ansatz* can not be studied independently, since they affect each other. For instance, optimal operator order will change from one reference state to another.

In this situation, we decided to start by testing the minimization process under different Trotter numbers, since we know from Eq. (7) that the error of the decomposition is inversely proportional to t . Both reference state and operator ordering will affect the performance

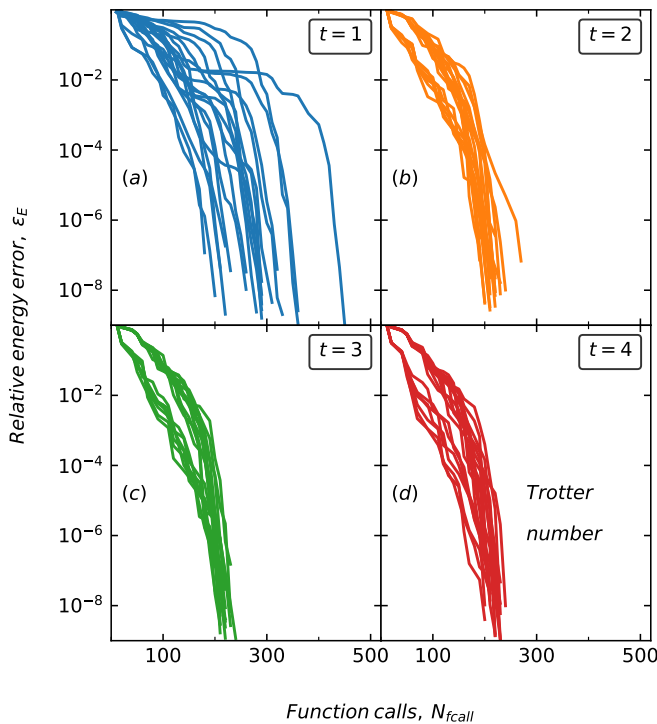


FIG. 2: Optimisation evolution for the relative error of the UCC energy function using the BFGS method. Each Panel shows 20 tracks of randomised operators ordering for different reference states using Trotter numbers from 1 to 4.

of the simulation. Thus, we simulate a large number of *ansätze* with different reference states from the basis and different operators orderings. In Fig. 2, we plot 20 of these simulations for each t , from $t = 1$ to $t = 4$.

As we see in the Panel (a) of Fig. 2, for Trotter number $t = 1$ some *ansätze* lead to sub-optimal minimisations, often taking more than $N_{fcall} = 300$ function calls before reaching $\epsilon_E = 1 \times 10^{-9}$. In contrary, in the other Panels we see that higher Trotter numbers usually lead to fewer function calls, between 200 and 250. However, there is no substantial improvement from $t = 2$ to $t = 4$. We use $t = 2$ from now on, since higher Trotter numbers lead to more costly simulations.

To test the effect of the reference state on the UCC method, we use a large number of random operator orderings for each determinant of the basis. Particularly, perform the UCC method for 2000 different *ansätze*, shuffling the order of the operators (without repeating) in the exponential. The average \bar{N}_{fcall} for each *ansatz* is shown in Table III.

The difference between the states is not very significant. However, we can notice that the degenerated states perform very similar and states with lower energies are not necessarily better than the more energetic ones.

A property that seems to be related with the efficiency of the state is the infidelity. In general, states with lower infidelity (or higher overlap) need less N_{fcall} than the

$ v_i\rangle$	E_i	I_i	2000 samples
			$\bar{N}_{fcall} \pm \delta$
$ v_1\rangle$	2.58	1.00	218 ± 14
$ v_2\rangle$	1.14	0.83	209 ± 11
$ v_3\rangle$	2.58	1.00	217 ± 14
$ v_4\rangle$	1.14	0.83	210 ± 12
$ v_5\rangle$	0.67	0.86	201 ± 10
$ v_6\rangle$	1.14	0.83	209 ± 11
$ v_7\rangle$	-0.75	0.98	212 ± 11
$ v_8\rangle$	1.14	0.83	210 ± 11
$ v_9\rangle$	-0.75	0.98	212 ± 11
$ v_{10}\rangle$	0.67	0.86	201 ± 10

TABLE III: Average number of function calls (\bar{N}_{fcall}) of the minimisation for each state of the basis using 2000 different operator orders with the corresponding standard deviation (δ). The first three columns show the state used in the simulation along with its energy (E_i) and infidelity (I_i).

others. Notice that the infidelity (or overlap) of the reference state is not something we can know before starting the simulation. Some works suggest using the Hartree-Fock state [13, 14], which should have higher overlap than the states of the basis. From now on we use $|v_{10}\rangle$, one of the states that needed fewer N_{fcall} .

Next, we are going to take a look at the possible ordering of the operators in the exponential Trotter decomposition. As we discussed before, the ordering of the excitation operators in the exponential can change the *ansatz* outcome, so it is interesting to check if some combinations lead to faster simulations. Other studies suggest that the ordering the operators according on their amplitudes in the Hamiltonian leads to more efficient simulations [14].

Since the operators we are working with are basically the two-body contributions of the Hamiltonian, we can use the \bar{v}_{ijkl} matrix element to quantify their "amplitudes". Doing so, we can structure the Trotter decomposition in an ascending or descending order depending on the \bar{v}_{ijkl} terms.

In the ascending order, the "less important" operators are applied first to the reference state, while in the descending order the "more important" are the first ones. To check the performance using this criterion, we compare this two *ansätze* with several randomized ones in Fig. 3.

The results show little difference in performance comparing the minimisation process of different *ansätze*. As we see in Fig. 3, there are several random orderings that need less function calls. With this particular basis and operator pool, ascending or descending ordering does not lead to significant efficiency improvements.

V. CONCLUSIONS AND OUTLOOK

In this work we study the different aspects of the UCC *ansatz* and their effect on the efficiency of the method

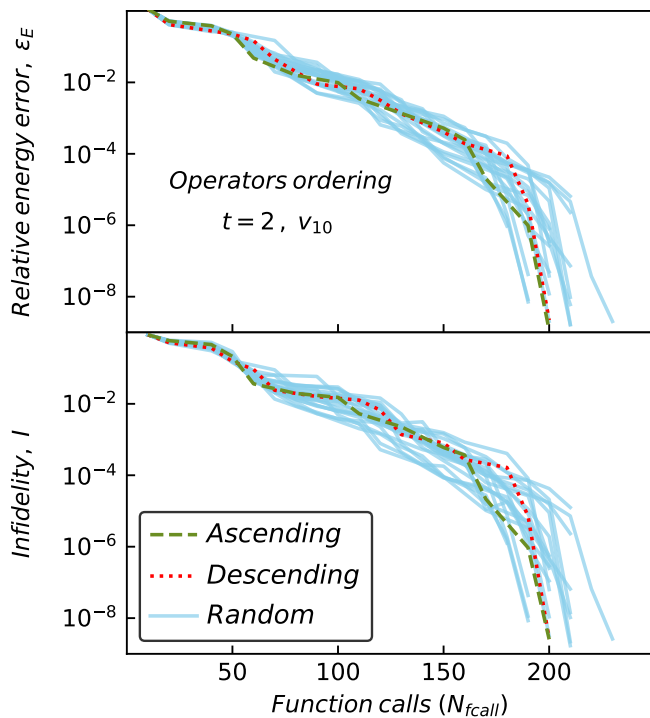


FIG. 3: Evolution of the relative error for the ground-state energy (ϵ_E) and the infidelity (I) as a function of the number of function calls (N_{fcall}). The manually chosen ascending and descending orders for the operators are shown with dashed and dotted lines, respectively. Random configurations are shown with solid lines.

simulating the ${}^6\text{Li}$ nucleus. The default *ansatz* uses 45 operators and the first state of the basis ($|v_1\rangle$) as the reference state. The simulation is successful and the minimiser need $N_{fcall} = 1288$.

First, we reduce significantly the number of operators we use from the pool, by simply discarding the ones that have no effect on the reference state. This translates to fewer N_{call} thanks to the reduction of parameters θ .

Second, we compare the performance of different Trotter numbers using every single state of the basis with a large number of randomised operator sequences. We show how the Trotter number $t = 1$ can lead to inefficient simulations. Thus, we consider using $t = 2$, since its more stable output.

Subsequently, we compute the average number of iterations needed for the optimiser to end the simulation for each state of the basis. 2000 different random operator orders are used for each state to make this calculus, showing how the energy of the states are not related with their performance. Instead, the main property of the reference state that leads to better performance is its overlap with the ground state. This information is not available before an actual estimation of the ${}^6\text{Li}$ ground state energy.

Finally, we try to establish a criterion regarding the ordering of the operators in the exponential decomposition. We use randomized and manually selected configurations, taking into account the amplitudes of the operators in the Hamiltonian, to compare their performance. This choices do not performe significantly better compared to the random ones.

There is more room for improvement when it comes to the UCC method. An in-depth study of the order of the operators in the *ansatz* should be done in order to fully understand its effect on the simulation. Also, some approximations can be used to obtain high-overlap reference states, which seems promising for the efficiency of the method. Overall, the UCC method has proven to be a very powerful tool for nuclear physics that will have its impact in the future of quantum computing.

Acknowledgments

First, I would like thank my advisor, Arnau Rios, for his guidance and support through the entire process. I also want to thank Javier and Antonio, for their huge contribution to this work and my family and friends, the best company one can ask for.

-
- [1] D. Deutsch and R. Jozsa. Proc. R. Soc. Lond. A 439:553–558(1992).
- [2] R. Feynman, Int. J. Theor. Phys. 21, 467 (1982).
- [3] A.M. Romero, J. Engel, H. L. Tang and S. E. Economou, Phys. Rev. C 105, 064317 (2022).
- [4] K. Choi, D. Lee, J. Bonitati, Z. Qian and J. Watkins, Phys. Rev. Lett. 127, 040505 (2021).
- [5] M. G. Mayer, Phys. Rev. 75, 1969 (1949) .
- [6] K. Heyde, *The Nuclear Shell Model*, ed. Springer-Verlag Berlin, Heidelberg (1994)
- [7] E. K. U. Gross, E. Runge and O. Heinonen, *Many-particle theory*, ed. A. Hilger Bristol, Philadelphia (1991).
- [8] S. Cohen and D. Kurath, Nucl. Phys. 73, 1 (1965).
- [9] R. J. Bartlett and M. Musiał, Rev. Mod. Phys. 79, 291 (2007)
- [10] M. Nielsen and I. Chuang, *Quantum Computation and Quantum Information*, ed. Cambridge University Press, Cambridge (2010).
- [11] M. Suzuki, Commun.Math. Phys. 51, 183–190 (1976).
- [12] F. Ajzenberg-Selove, Nucl. Phys. A 490, 1, (1988).
- [13] A. Anand P. Schleich, S. Alperin-Lea, P. Jensen, S. Sim, M. Díaz-Tinoco, J. Kottmann, M. Degroote, A. Izmaylov and A. Aspuru-Guzik Chem. Soc. Rev. 51, 1659–1684 (2022)
- [14] O. Kiss, M. Grossi, P. Lougovski, F. Sanchez, S. Vallecorsa and T. Papenbrock, Phys. Rev. C 106, 034325 (2022).